# Supplemental Information

## Near Room Temperature Multilevel Resistive Switching Memory with Thin Film Ionic Liquid Crystal

*Wenzhong Zhang, Shingo Maruyama*, Kenichi Kaminaga, Yuji Matsumoto*

Department of Applied Chemistry, Graduate School of Engineering, Tohoku University, Sendai 980-8579, Japan

*Corresponding author: Shingo Maruyama ; E-mail: maruyama-s@tohoku.ac.jp

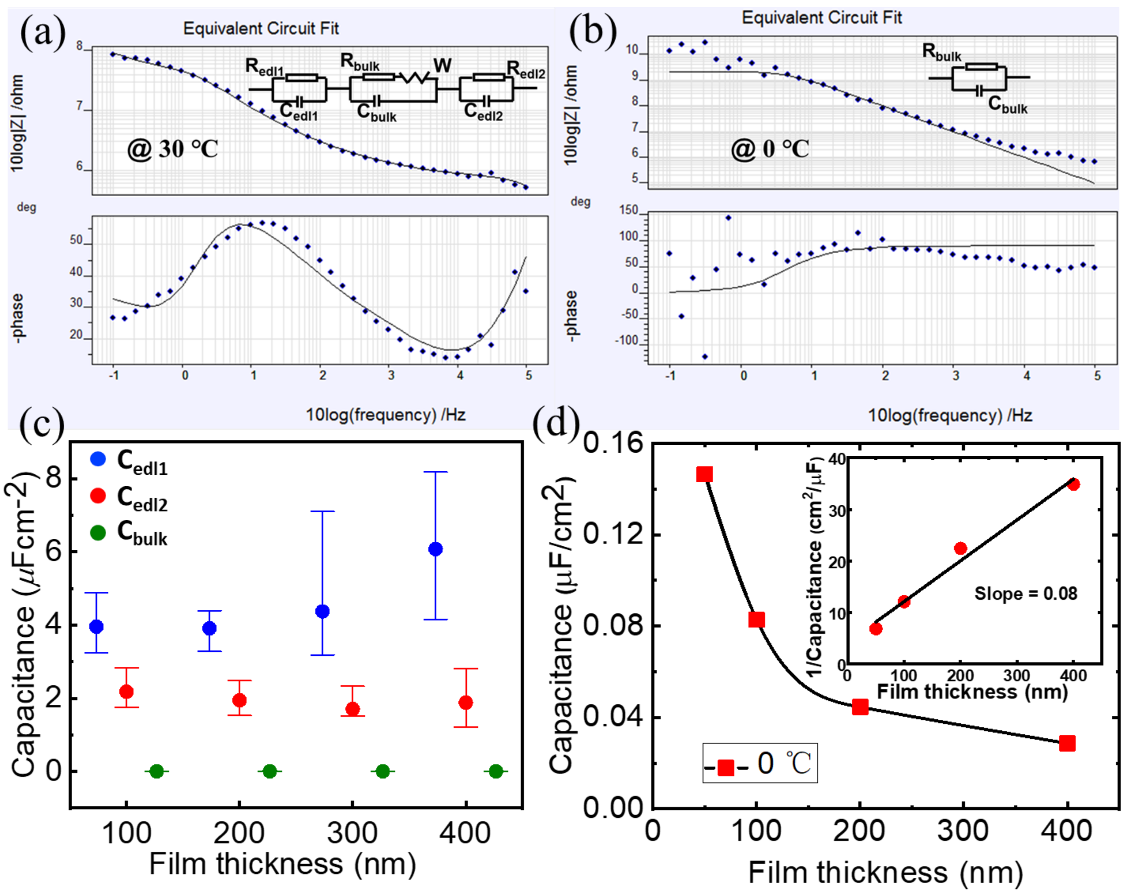


**Figure S1.** Bode plots of EIS for the Ag/[$C_{12}$mim][$BF_4$]/H-Si(100) devices taken without bias voltages at (a) 30 °C and (b) 0 °C. The blue diamonds and the black solid lines indicate the experimental data and their fittings, respectively. The insets are the equivalent circuit models used for the fitting, where one model including two parallel RC circuits and one parallel RC circuit with Walburg component (W) in series was for the fitting at 30 °C, the other model with one parallel RC circuit was used at 0 °C. The values of $C_{edl1}$ and $C_{edl2}$ at 30 °C are 2.37 and 2.67 $\mu$ F/cm$^2$, respectively, which are acceptable values for the EDL capacitance, with a $C_{bulk}$ of 0.006 μF/cm$^2$ which can be ignored. In contrast, the value of $C_{bulk}$ at 0 °C is 0.05 μF/cm$^2$, which is too small as the EDL and is only a value of bulk insulator capacitance, indicating that the EDL was not formed at 0 °C. Thickness dependence of the capacitance measured at (c) 30 °C (SmA phase) and (d) 0 °C (LtSm or crystal phase) of a Ag/[$C_{12}$mim][$BF_4$]/H-Si(111) device. The inset of (d) shows a plot of the inverse of capacitance against the thickness. The fitting of the experimental data is depicted as a solid line. The capacitance was inversely proportional to the thickness at 0 °C, while the capacitance became independent of the thickness at 30 °C, indicating that an electric double layer (EDL) is formed at the electrode interfaces when thin film [$C_{12}$mim][$BF_4$] is in the SmA phase.[1] These relationship between the capacitance and ILC film thickness confirmed the formation of EDL when thin film [$C_{12}$mim][$BF_4$] is in the SmA phase.

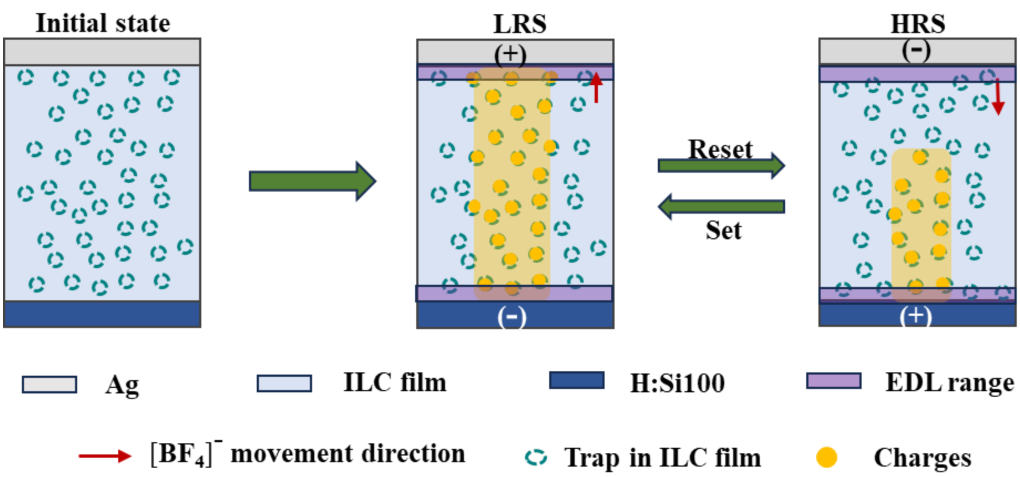


**Figure S2.** Schematic illustration of the device operation at 30 °C. When a positive voltage was applied between the top and bottom electrodes, the EDLs were formed at the interfaces between [$C_{12}$mim][$BF_4$] and the electrodes by the movement of ions near the interface, which would allow for a large electrical field concentrated at the interfaces, assisting the injection of charges from the electrodes into the $[C_{12}mim][BF_4]$ layer. Once the charges are injected, they would be trapped by the ions. In the set process, the formation of CFs proceeds with the traps gradually filled under such a positive voltage applied, leading to the LRS of the device. In the reset process, as a reverse voltage is applied between the electrodes, the polarity of the EDLs at the interfaces become opposite, and the trapped charges are gradually de-trapped, with the eventual rupture of the CFs returning the device to the HRS.

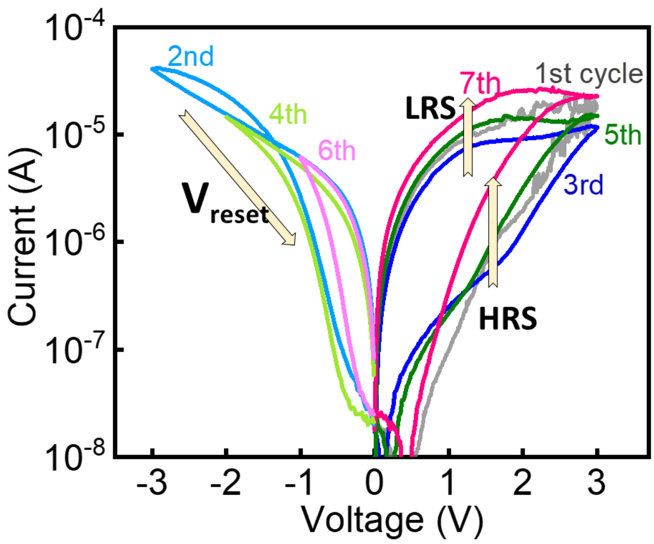


**Figure S3.** Reset voltage ($V_{reset}$) dependence of $I$–$V$ curves. The order of the voltage sweep is indicated by the ordinal number along side of each curve. The currents of the HRS and LRS in the positive voltage sweeps (set process) increased as $V_{reset}$ decreased.

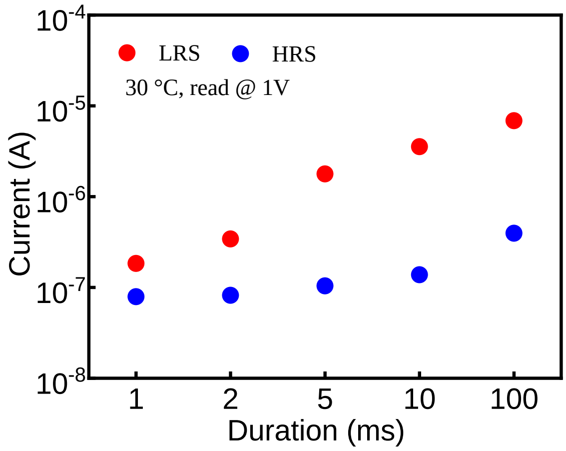


**Figure S4.** Duration dependence of the respective current values read at +1 V in the LRS and HRS taken from Figure 4b.

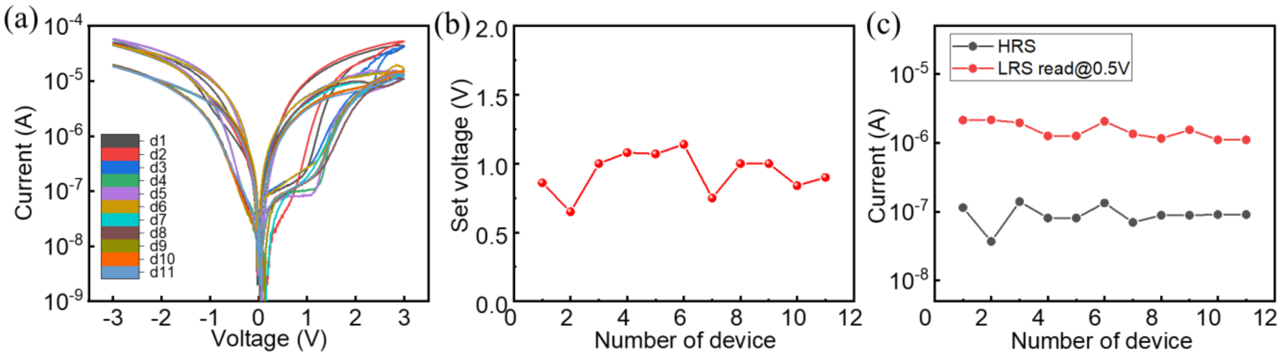


**Figure S5.** (a) *I*–*V* curves of randomly selected devices, (b) & (c) Variations of the set voltage, and of the current value for the LRS and HRS read at 0.5V, extracted from (a). The set voltage value was varied around 0.9 V with a standard deviation of ± 0.1 V. The respective current values at the LRS and HRS showed small variations: $1.6 \pm 0.3 \times 10^{-6}$ A for the LRS and $9.3 \pm 1.9 \times 10^{-8}$ A for the HRS.

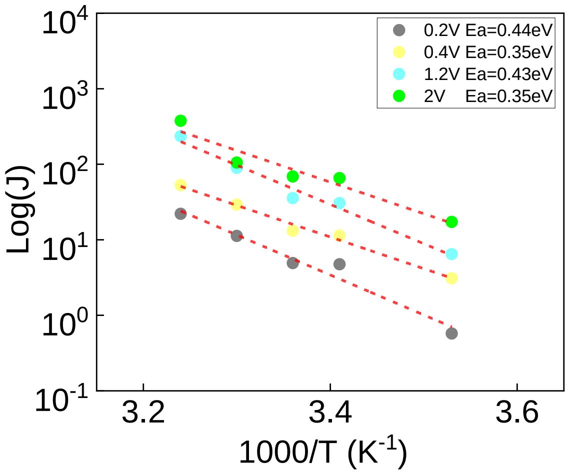


**Figure S6.** Arrhenius plots for the *I–V* curves at different voltages in Figure 3c.

**Table S1.** Comparison of ReRAM devices using various switching layer materials.

| Top/Bottom Electrodes | Switching layer | Switching voltage (V) | Endurance (cycles) | Retention (s) | Multilevel/ Neuromorphic operation | Ref. |
|---|---|---|---|---|---|---|
| Cu/Pt | ($[C_4mim][Tf_2N]$: $Cu[Tf_2N]_2$)-$HfO_2$ | 0.9 | 50 | - | - | [1] |
| Cu/Cu | $[C_4mim][Br]$:$H_2O$ | ~1 | 1000 | - | Multilevel | [2] |
| Cu/Cu | ($PAA^-$ $Na^+$:$H_2O$):(NaOH) | - | 500 | 10000 | Neuromorphic | [3] |
| Ag/Si | $[C_{16}mim][PF_6]$ | 0.6 | 44 | 1000 | - | [4] |
| Ag/Si | $[C_{12}mim][BF_4]$ | 1 | 50 | 2000 | Multilevel | this result |
| Au/ITO | $Cu_3(HHTP)_2$ | 1 | 10000 | 10000 | - | [5] |
| Ag/Pt | IGZO | 0.9 | 100000 | 10000 | - | [6] |
| Ag/Pt | PEO/PVK | 1 | 100 | 100000 | - | [7] |
| Ag/Ag | Ag-GeTe | 0.18 | - | 100000 | Multilevel & neuromorphic | [8] |
| Cu/Pt | $HfO_2$ | 2 | - | - | - | [9] |
| TiN/Ta | $Ta_2O_5$ | -1~-3 | - | - | Multilevel & neuromorphic | [10] |
| Ag/ITO | P3HT:PCBM | 0.5~2.9 | 100 | - | Multilevel | [11] |

**Supporting References**


1. Komatsu, H.; Tanaka, M.; Kaminaga, K.; Maruyama, S.; Matsumoto, Y. Electric Double Layer Action of High-Quality Ionic Liquid Crystal Thin Films. Chem. Lett. 2022, 51 (2), 162–165.
2. K. Kinoshita, A. Sakaguchi, A. Harada, H. Yamaoka, S. Kishida, Y. Fukaya, T. Nokami, T. Itoh, Jpn. J. Appl. Phys., 2017, 56 (4S), 04CE13.
3. M.Y. Chougale, S.R. Patil, S.P. Shinde, S.S. Khot, A.A. Patil, A.C. Khot, S.S. Chougule, C.K. Volos, S. Kim, T.D. Dongale, Ionics, 2019, 25, 5575–5583.
4. M.U. Khan, G. Hassan, J. Bae, J. Mater. Chem. C, 2020, 8, 13368-13374
5. W. Zhang, H. Komatsu, S. Maruyama, K. Kaminaga, Y. Matsumoto, ACS Appl. Mater. Interfaces, 2023, 15(45), 52806–52813
6. L. Liu, J. Dong, J. Liu, Q. Liang, Y. Song, W. Li, S. Lei, Small Struct., 2021, 2: 2000077.
7. A. Ali, Y. Abbas, H. Abbas, Y.-R. Jeon, S. Hussain, B.A. Naqvi, C. Choi, J. Jung, Appl. Surf. Sci. 2020, 525, 146390.
8. H.-M. Seung, K.-C. Kwon, G.-S. Lee, J.-G. Park, Nanotechnology, 2014, 25, 435204.
9. M.J. Yu, K.R. Son, A.C. Khot, D.Y. Kang, J.H. Sung, I.G. Jang, Y.D. Dange, T.D. Dongale, T.G. Kim, JMR&T, 2021, 15, 1984-1995.
10. M. Haemori, T. Nagata, T. Chikyow, Appl. Phys. Express, 2009, 2, 061401.
11. D. S. Kuzmichev, A. M. Markeev, Nanobiotechnology Reports, 2021, 16(6), 804-810
12. S. Gao, F. Zeng, C. Chen, G. Tang, Y. Lin, Z. Zheng, C. Song, F. Pan, Nanotechnology, 2013, 24, 335201.